LA-UR -84-4025

Conf-850466--1

Los Alamos National Laboratory is operated by the University of California for the United States Department of Energy under contract W-7405-ENG-36

TITLE: AN INVESTIGATION INTO THE HIGH STRAIN-RATE BEHAVIOR OF COMPACTED SAND USING THE SPLIT-HOPKINSON PRESSURE BAR TECHNIQUE

LA-UR--84-4025

DE85 005560

AUTHOR(S): C. W. Felice (USAF)
J. A. Brown (ESS-3)
E. S. Gaffney (ESS-5)
J. M. Olsen (U. Utah)

SUBMITTED TO: 2nd Symposium on the Interaction of Non-nuclear Munitions with Structures, 15-19 April 1985, Panama City Beach, FL.

Los Alamos

Los Alamos National Laboratory
Los Alamos, New Mexico 87545

FORM NO 836 R4
ST NO 2629 5/81

AN INVESTIGATION INTO THE HIGH STRAIN-RATE BEHAVIOR OF COMPACTED SAND USING THE SPLIT-HOPKINSON PRESSURE BAR TECHNIQUE

C. W. Felice*, J. A. Brown+, E. S. Gaffney+ and J. M. Olsen‡

*Capt., USAF, Air Force Institute of Technology, Wright-Patterson AFB, OH 45433
+Earth and Space Sciences Division, Los Alamos National Laboratory, Los Alamos, NM 87545
‡University of Utah, Salt Lake City, UT 84112

ABSTRACT

The results of compressive high strain-rate experiments on compacted sand are presented. Experiments were conducted on a 60.3 mm split Hopkinson pressure bar (SHPB). The experiments showed that the assumptions necessary for a valid SHPB experiment are satisfied when using compacted sand samples constrained to a nearly uniaxial strain state. Results show that the sample stress-strain response is governed principally by the initial sample gas porosity, and that no strain-rate dependence is exhibited at sample strains less than the initial gas porosity. Several stress-strain curves are presented for samples prepared at several combinations of moisture content and density with applied stresses and strain rates up to 520 MPa and 4000 sec^{-1}, respectively.

INTRODUCTION

This paper presents the results of a laboratory investigation into the high strain-rate behavior of compacted soil using the split Hopkinson pressure bar (SHPB) technique [1]. This work has been performed using a 60.3 mm SHPB which is located at the Los Alamos National Laboratory, Los Alamos, New Mexico [2].

For the experimental program, samples were statically compacted into thick-walled confining cylinders at lengths of 6.35 mm and 12.7 mm. The thick-walled confining cylinder provided a means of containing the sample and producing a condition of nearly uniaxial strain during the experiment. The compaction moisture and density combinations ranged from drier than to wetter than optimum conditions as determined by the Harvard compaction test. The applied stresses and strain rates ranged from 140 MPa to 520 MPa and 1000 sec^{-1} to 4000 sec^{-1}, respectively.

CONFINING SYSTEM

To achieve a nearly uniaxial strain environment for the experiments, the soil samples were compacted into thick-walled bearing-bronze cylinders. The dimensions of these cylinders were 60.35 mm inside diameter, 102 mm outside diameter, and 44.5 mm in length. These confining cylinders served two purposes; first, to contain the soil sample itself, and second, to cancel the effects of radial inertia, forcing the sample to experience a state of nearly uniaxial strain. Thus, sample distortion or barrelling was prevented by the elimination of friction at the specimen/bar interfaces.

When the confining cylinder containing the sample was placed in the bars, approximately 19 mm of the cylinder overlapped the bars on each end. To determine if the confining cylinder was transferring any stress to the transmitter bar, a test was conducted with the bars separated a distance of 3.0 mm (a distance greater than the anticipated displacement of the incident bar) and the confining cylinder placed over the air gap between the bars. If the confining cylinder did transfer stress to the transmitter bar a signal would be recorded at the transmitter bar strain gage; if not, the strain gage record would be flat. The results indicated that the confining cylinder did not transfer any measurable stress to the transmitter bar.

SAMPLE PREPARATION

The clayey sand (SC, Unified Soil Classification System) was obtained in bulk quantities from the McCormick Ranch test site located on Kirtland Air Force Base (KAFB), New Mexico. In order that the soil be as free of organic material as possible, the surface vegetation was removed and the samples were taken at a depth of 1 to 2 meters. After arriving at the University of Utah soils laboratory, the material was slaked to achieve a uniform mixture as well as to break apart large clumps of soil.

The majority of samples were prepared near the optimum moisture content (13.3%) and dry density (1.87 g/cc) as determined by the Harvard miniature compaction test (see Figure 1). To achieve as uniform conditions among samples as possible, the soil was mixed in batches of enough material to prepare a minimum of five experimental samples. Before the addition of water, the soil was passed through a No. 4 sieve (4.75 mm opening). The soil was then carefully weighed and placed in a large flat pan. The correct amount of moisture was added by using a spray bottle so that an even distribution could be obtained. The sample material was then mixed thoroughly. After mixing, a damp cover was placed over the soil for a period of 20 minutes to allow the soil-water mixture to stabilize. Following the stabilization period, the sample was again mixed to ensure that an even mixture was obtained.

MASTER

The individual experimental samples were then prepared by removing the appropriate soil mass from the batch mix to yield a given volume when compacted. The samples were statically compacted in the confining cylinders by using a hydraulic press with spacer rings to control the sample length (and hence, density). Two sample lengths were used: 12.7 mm and 6.35 mm. Each sample was then sealed in a plastic bag to reduce any moisture loss that might occur prior to the actual experiment. The same procedure was followed for samples prepared on the wet and dry side of optimum conditions.

EXPERIMENTAL PROGRAM

The information reported here represents the results of twenty-six experiments. In most cases, a minimum of two experiments were conducted at each combination of moisture content and density, in order that data replication could be obtained. Due to the nature of the specific Hopkinson bar apparatus used, the seating strains could not be controlled with great accuracy, hence the pre-experiment sample length differed from sample to sample affecting the ability to achieve exact experiment replication. In addition, there existed a friction force between the launch tube and the striker bar such that it was difficult to achieve duplicate impact velocities. The applied stresses (i.e., the amplitudes of the incident waves in the bar) ranged from 240 MPa to 520 MPa. At the completion of the experiment, the sample was removed from the confining cylinder and a post-experiment moisture content determined.

EXPERIMENTAL ASSUMPTIONS

In analysing the strain gage data recorded in the SHPB experiment, several assumptions need to be addressed. These are:

1) That there exists a uniform distribution of axial stress over the length of the sample;

2) That there exists a uniform distribution of radial stress over the length of the specimen;

3) That the interfaces between the bars and the samples are frictionless.

Assumptions two and three will be addressed first, followed by assumption one.

A nearly uniaxial strain state is forced upon the sample by the fact that it is contained in a thick-walled confining cylinder. As the nominal inside diameter of the confining cylinder is the same as the diameter of the bar, the stress applied to the sample will be constant across the sample diameter (provided that the stress is constant over the diameter of the bar) [2]. This configuration will also constrain the sample such that there will be no appreciable radial strain.

As briefly mentioned earlier, this configuration will prevent sample distortion or barreling during the experiment. In the traditional SHPB experiment a sample with a diameter slightly less than that of the bars is placed between them. This is to allow the sample to expand radially during the experiment while not exceeding the diameter of the bar. As stress is applied to the sample, radial shear forces are created between the bars and the sample. These have commonly been referred to as "end effects" or "friction effects." A result of these end effects is that the sample tends to be clamped at the specimen/bar interfaces [3]. This prevents the sample from expanding uniformly; hence, barreling of the sample is observed. By preparing the sample at the same diameter as that of the bars and confining it so that no radial expansion is allowed, these "end effects" are eliminated.

An analytic method for determining when stress uniformity is achieved in an SHPB sample was developed by Davies and Hunter [4] based on energy considerations and use of the Taylor-von Karman theory for the plastically deforming sample. This expression is written as follows:

$$\frac{d\sigma}{d\epsilon} > \frac{\pi^2 \rho_s l^2}{T^2}$$

where $d\sigma/d\epsilon$ is the slope of the stress-strain curve, ρ_s is the density of the specimen, l is the length of the specimen, and T is the time required for the stress to equilibrate in the sample. Figure 2 shows results from a typical experiment. Using the above expression with the stress-strain curve (Fig. 2a) and the appropriate sample length and density, T is computed to be 66 microseconds. From Fig. 2b, it can be determined that after about 65 microseconds the stresses at the two interfaces are indeed approximately equal. The stress difference across the interfaces as a function time is shown in Fig. 2c. If axial inertia forces are absent, this stress difference should be zero. It can be seen that after about 65 microseconds the stress difference is very small.

EXPERIMENTAL RESULTS

Figures 3 and 4 show typical stress-strain curves for sample lengths of 12.7 mm and 6.35 mm, respectively, over a range of applied stresses. The experimental conditions are given in Table 1. In both figures, the initial portions of the curves are slightly concave toward the stress axis. The average stress experienced by the specimen increased with increasing applied stress independent of the sample length. The stress-strain response was very similar for applied stresses up to 400 MPa with some increase in stiffness observed at higher applied stresses. For all applied stress levels, the samples began to stiffen at strains approximately equal to the gas porosity. For both sample lengths and at all applied stresses, the strain at peak stress experienced by the sample exceeded the gas porosity of the material. This discrepancy will be addressed in the next section.

To observe how moisture content variations affect the stress-strain response of the soil, samples were prepared at the following nominal moisture contents; 7 percent, 13 percent and 15 percent (see Figure 1 for relationship to the Harvard compaction curve). Figures 5 and 6 show the effect of moisture content on stress-strain response for sample lengths of 12.7 mm at an applied stress of 400 MPa, and 6.35 mm at an applied stress of 250 MPa, respectively. From Figure 5, there is a clear indication that the average stress experienced by the samples increased with

TABLE 1
Summary of experimental conditions.

Experiment Number	Sample length (mm)	Water content (%)	Gas porosity (%)	Wet density (Mg/m^3)	Applied stress (MPa)
112	6.44	11.8	7.9	2.09	425
113	6.45	12.1	7.7	2.09	385
114	6.55	12.1	9.2	2.05	386
115	6.45	11.4	10.6	2.04	395
116	6.37	11.2	8.1	2.10	243
117	6.35	10.7	8.5	2.10	268
118	6.45	10.6	10.3	2.07	244
119	6.45	10.4	9.9	2.08	246
131	13.13	12.4	9.6	2.04	387
132	12.69	12.5	6.9	2.10	375
133	12.91	12.4	8.0	2.07	368
134	12.59	12.4	5.8	2.12	399
135	13.07	7.0	23.4	1.84	385
136	12.23	15.1	5.2	2.08	397
138	5.96	13.0	4.9	2.13	251
139	6.09	7.0	17.7	1.98	249
145	12.65	11.8	6.2	2.13	269
146	12.67	11.9	6.3	2.13	523
147	6.36	11.9	6.6	2.12	237
148	6.31	14.4	7.4	2.04	249
162	6.29	13.0	4.4	2.14	519
163	6.31	12.9	4.8	2.13	522
164	12.98	12.9	7.5	2.07	507
165	12.89	12.7	7.1	2.09	254
166	6.24	14.0	4.4	2.12	261
167	6.22	14.0	4.1	2.12	261

increasing moisture content (Table 1). Also the samples became stiffer with increasing moisture content, and the strain at peak stress experienced by the sample decreased with increasing moisture content. As with the other stress-strain curves shown, there is a marked break in slope near the gas porosity. This change is slope is not observed for the dry sample (experiment 135). The strain experienced by the sample at peak stress decreased with increasing water content. The 6.35 mm samples also became stiffer with increasing moisture content with a change in slope near the gas porosity (Figure 6). However, this change in slope is less abrupt than observed in the thicker samples. As with the 12.7 mm sample, the 6.35 mm samples experienced decreasing strain at peak stress with increasing moisture content.

There is a difference in the response of the dry sample for the two sample lengths. The 12.7 mm sample, which had a gas porosity of 23.4 percent, experienced very little build up of stress at the maximum strain of 16 percent. For the 6.35 mm sample, which had a gas porosity of 17.7 percent, the accumulated strain approached that value with a substantially higher build up of stress. Therefore, it appears that stiffening begins at strains slightly less than the initial gas porosity.

Another major interest of this research was whether or not a sufficient degree of experimental replication could be achieved. Figure 7 demonstrates the success of this effort. There is virtually no observable difference between the four experiments in this figure, except that one sample (experiment 117) received an impact stress somewhat higher than the other three.

To determine the strain-rate sensitivity of the compacted soil, stress-strain rate curves were constructed at constant strain levels. Such a plot is shown in Figure 8 for 6.35 mm samples compacted to moisture and density conditions near optimum. The dashed lines show the stress-strain rate trajectories averaged for each of two sets of experiments conducted at the same applied stress. The solid lines connect points of constant strain between the two sets. From Figure 8, it can be seen that there is no strain-rate dependence at strains less than the initial gas porosity. This is in accord with the findings of Gaffney <u>et al.</u> [2] that strain-rate dependence effects on <u>loading</u> occurred in dry alluvium only at strain rates above 5000 sec^{-1}.

DISCUSSION

In most cases, the strains experienced by the samples exceeded the initial gas porosity. Several phenomena may work together to account for this observed discrepancy: 1) Water compression, 2) Radial expansion of the confining cylinder, 3) Water loss, and 4) Soil loss. The first three have the potential to be examined quantitatively, while the last can be looked at qualitatively, at best. Addressing the potential strain contribution of the above factors individually and then summing their contributions would seem a natural approach to the problem. However, the experimental environment complicates this approach. At the incident bar/sample interface the initial compressive stress wave is reflected as a tensile wave due to the lower impedance of the sample relative to the bar. This tensile wave travels back down the bar toward the end at which impact occurred. As the impact end of the bar is now a free end, the tensile wave is reflected as a compressive wave travelling once again toward the sample, and hence, reloading the sample. Because of this multiple impact situation, there is no way to determine the contribution from water loss and soil loss during the period of the first applied pulse alone (about 150 μs).

Because a sample moisture was determined before and after each experiment, a measure of the amount of moisture loss is available. The average moisture loss for all the experiments was 11.0 percent. Also, it can be observed that some soil mass is lost from the confining cylinder during the experiment. However, there is no way of measuring how much is lost or the distribution of the loss (if the loss occurs during the period of the first applied pulse or later in the experiment). It is also certain that the pore water does compress and the confining cylinder does experience radial expansion.

Because of the uncertainty in the evaluation of the strain contribution from the above-mentioned factors individually, a gross strain adjustment has been made even though it is possible to calculate the effect of water compression and cylinder expansion. This was accomplished by plotting the difference between the strain at maximum average stress and the initial gas porosity against the average force (computed as the maximum average stress multiplied by the area of the sample). A simple linear regression line was then fit to the data for samples prepared near optimum water content (Figure 9). Using the regression line and the average force experienced by the sample, a systematic strain correction was then computed for each experiment. The strain correction was then added to the sample gas porosity to yield an accountable sample strain which could be compared to the strain experienced by the sample at the maximum average stress. The discrepancy between the accountable strain and the strain at maximum stress is then used as a measure of the success of the correction (Table 2).

TABLE 2

Accountable strain for sample at optimum conditions

Test No.	Gas porosity (%)	Strain correction (%)	Sum (%)	Strain at peak stress (%)	Balance (%)
112	7.9	7.87	15.77	19.79	4.02
113	7.7	7.67	15.37	17.40	2.03
114	9.2	7.61	16.81	19.60	2.79
115	10.6	8.07	18.67	18.03	-0.64
116	8.1	4.98	13.08	14.24	1.16
117	8.5	6.54	15.04	14.50	-0.54
118	10.3	5.18	15.48	14.06	-1.42
119	9.9	4.93	14.83	14.07	-0.76
131	9.6	6.10	15.70	12.68	-3.02
132	6.9	6.43	13.33	10.67	-2.66
133	8.0	5.52	13.52	12.52	-1.00
134	5.8	6.57	12.37	12.22	-0.15
138	4.9	5.75	10.65	11.80	1.15
145	6.2	3.51	9.71	10.12	0.41
146	6.3	9.41	15.71	13.30	-2.41
147	6.6	4.78	11.38	12.99	1.61
162	4.4	9.74	14.14	20.60	6.46
163	4.8	12.52	17.32	15.27	-2.05
164	7.5	9.28	16.78	12.43	-4.35
165	7.1	2.70	9.70	9.27	-0.43

After making the strain adjustment, experiment 162 is the only experiment that has a significant discrepancy remaining. The stress-strain curve for that experiment (Figure 10) suggests that a greater amount of soil and water extrusion may have occurred in that experiment than in the other experiments. At about 270 MPa, the sample begins to accumulate strain with very small changes in stress. Similar behavior is not observed to this extent in any other sample, and we believe that it can be attributed to excessive extrusion of soil and water during the course of the experiment.

It was observed in Figure 8 that as the accumulated sample strain approached and exceeded the initial gas porosity a dependence on strain-rate seemed to develop. However, this apparent behavior should be viewed with some caution for two reasons. First, the constant strain curves used to show this apparent strain-rate dependence are only rough averages developed from a few data points. Second, the factors identified to account for the discrepancy between the strain at maximum stress and the initial gas porosity cannot be quantified with the necessary accuracy to determine their effect on the apparent strain-rate dependence.

CONCLUSIONS

From the results of this experimental study conducted on compacted sand samples at strain rates up to 4000 sec^{-1}, we draw the following conclusions.

a) The assumptions necessary for a valid SHPB experiment can be satisfied for compacted sand samples constrained to a nearly uniaxial strain state.

b) Experimental replication can be achieved if sufficient care is taken in sample preparation and generation of the incident stress wave.

c) The stress-strain response of the soil studied is governed principally by the initial gas porosity of the sample.

d) Compacted clayey sand samples appear to be insensitive to strain rate (at least up to 4000 sec^{-1}) so long as the strain experienced is less than the initial gas porosity. At strains in excess of that value, there is an apparent strain-rate dependence; however, caution is recommended until further experimental confirmation of this apparent behavior can be obtained.

REFERENCES

[1] Kolsky, H. An investigation of the mechanical properties of materials at very high rates of loading. Proc. Phys. Soc. B62, 676-700 (1949).

[2] Gaffney, E. S., J. A. Brown and C. W. Felice, Soils as samples for the split Hopkinson bar. This volume.

[3] Green, S. J., and R. D. Perkins, Uniaxial compression tests at strain rates from 10^{-4}/sec to 10^{4}/sec on three geologic materials. DASA 2199, Defense Atomic Support Agency (now Defense Nuclear Agency), Washington (1969).

[4] Davies, E. D. H, and S. C. Hunter, The dynamic compression testing of solids by the method of the split Hopkinson pressure bar. J. Mech. Phys. Solids 11, 155-179 (1963).

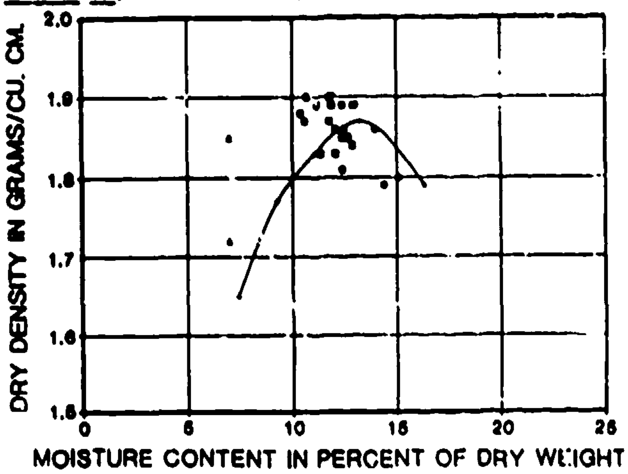

Figure 1. Sample moisture and density in comparison to the Harvard compaction curve. + Harvard compaction data, o wet of optimum, Δ dry of optimum, O near optimum.

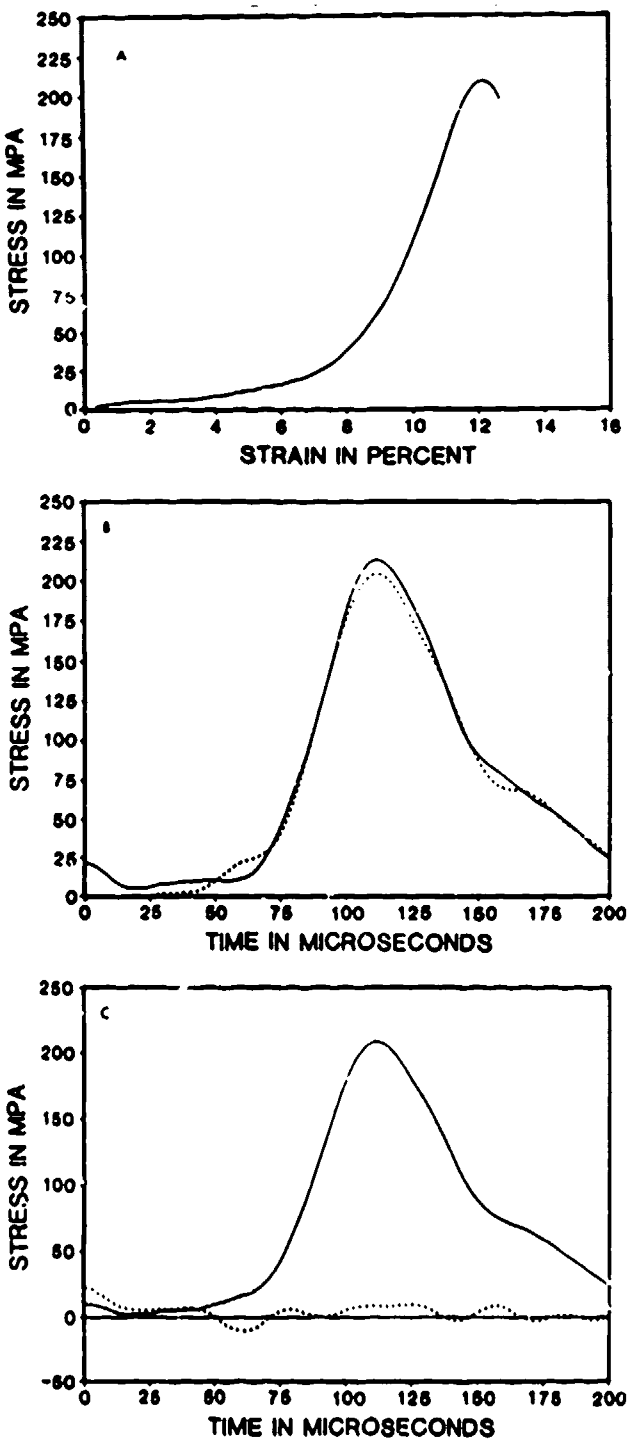

Figure 2. Typical experimental results for a 12.7 mm sample with an applied stress of 400 MPa.

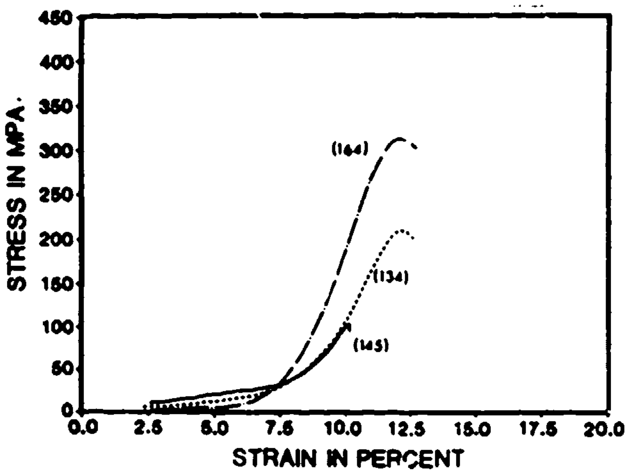

Figure 3. Experimental results for a 12.7 mm sample over a range of applied stresses. 269 MPa, solid; 399 MPa, dashed; 507 MPa, chain-dotted.

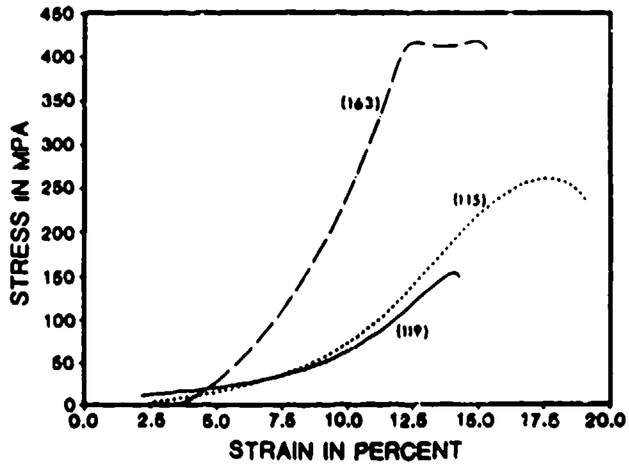

Figure 4. Experimental results for a 6.35 mm sample over a range of applied stresses. 246 MPa, solid; 395 MPa, dashed; 522 MPa, chain-dotted.

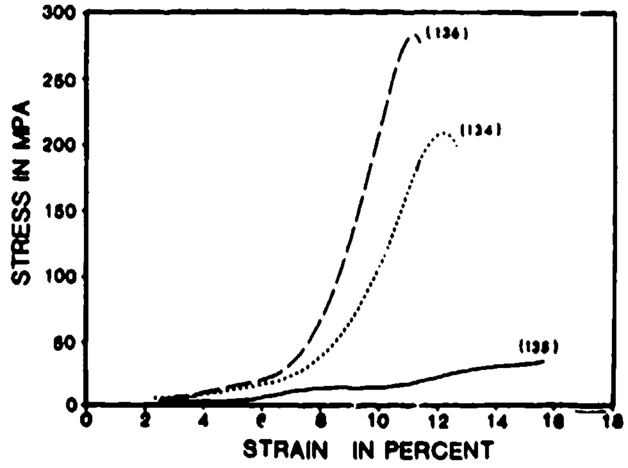

Figure 5. Experimental results for a 12.7 mm sample prepared at nominal moisture contents of 7 percent (solid), 13 percent (dashed) and 15 percent (chain-dotted).

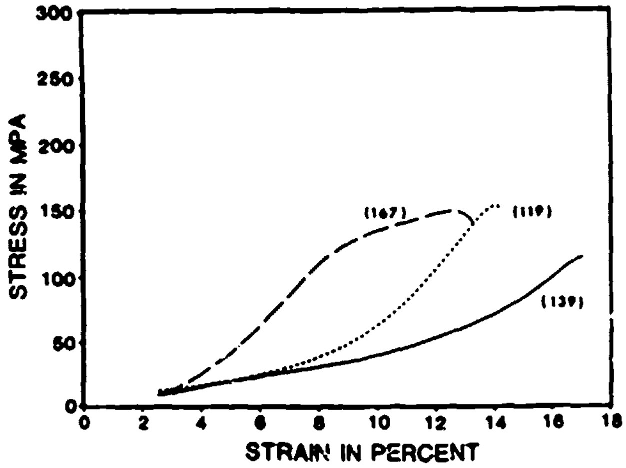

Figure 6. Experimental results for a 6.35 mm sample prepared at nominal moisture contents of 7 percent (solid), 13 percent (dashed) and 15 percent (chain-dotted).

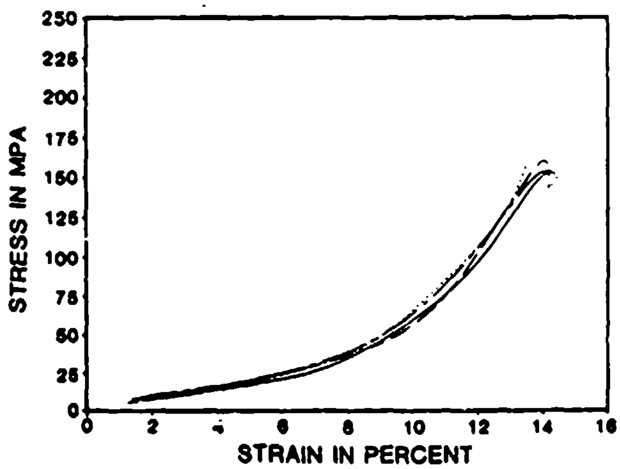

Figure 7. Experimental replication for 6.35 mm samples. The experiments are 116 (solid), 117 (dashed), 118 (chain-dotted), 119 (chain-dashed).

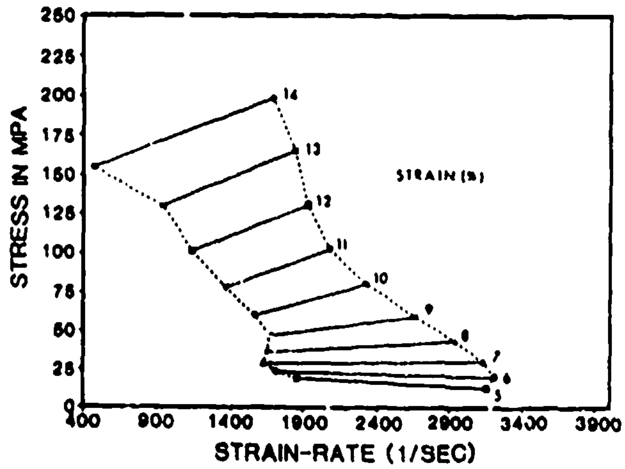

Figure 8. Stress-strain rate plot for 6.35 mm samples compacted to near optimum conditions.

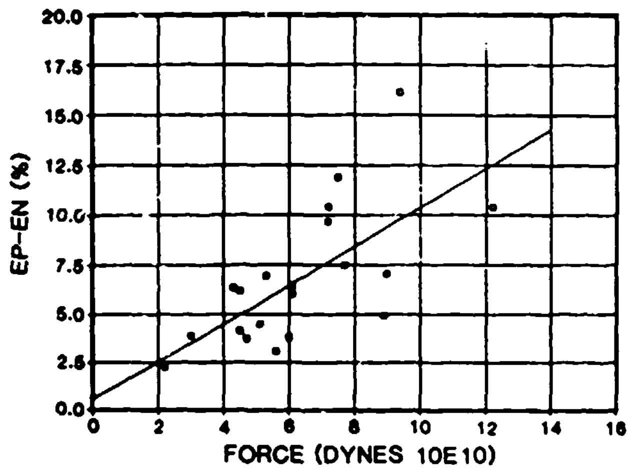

Figure 9. Linear regression fit to data for all samples compacted to near optimum conditions used in the systematic strain adjustment discussed in text.

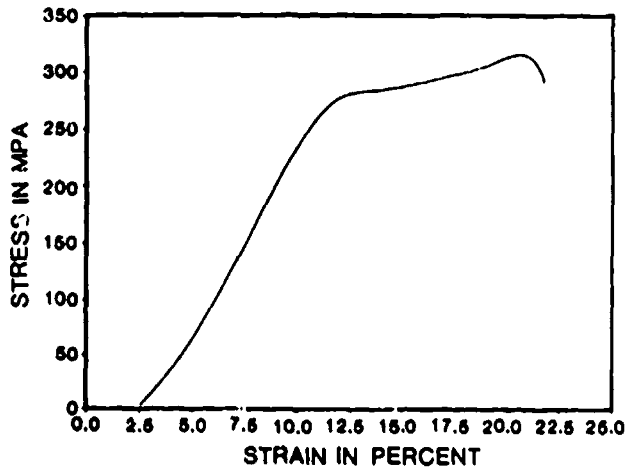

Figure 10. Stress-strain response for experiment 162.